

S. CIVIŠ<sup>1,✉</sup>  
P. KUBÁT<sup>1</sup>  
Z. ZELINGER<sup>1</sup>  
V. HORKÁ<sup>1</sup>  
A.N. IMENKOV<sup>2</sup>  
N.M. KOLCHANOVA<sup>2</sup>  
Y.P. YAKOVLEV<sup>2</sup>

## InAsSb/InAsSbP current-tunable laser with narrow spectral line width

<sup>1</sup> J. Heyrovský Institute of Physical Chemistry, Academy of Sciences of the Czech Republic, Dolejškova 3, 18223 Prague 8, Czech Republic

<sup>2</sup> Ioffe Physico-Technical Institute, RAS, 26 Polytechnicheskaya St., 194021 St. Petersburg, Russia

Received: 12 September 2002/Final version: 29 January 2003  
Published online: 22 May 2003 • © Springer-Verlag 2003

**ABSTRACT** The article describes the manufacture and testing of a new type of semiconductor laser working at low temperatures (12–100 K) in the wavelength range 3200–3300 cm<sup>-1</sup>. This kind of laser can be tuned in the modal range up to 6 cm<sup>-1</sup> and is characterized by a narrow spectral line width (about 7 MHz).

**PACS** 33.20 Ea; 42.55 Px; 07.57 Hm

### 1 Introduction

Laser spectroscopic methods have a number of advantages for the study of the absorption spectra of gaseous molecules in the laboratory and for in situ monitoring of harmful gases in the atmosphere. The use of lasers has significantly increased the detection sensitivity and selectivity in measuring weak signals of molecules with low absorbance or molecules at very low concentrations.

The development of new InAsSb/InAsSbP semiconductor lasers provides a tunable source of radiation with high spectral purity [1, 2]. These new types of lasers comply with the requirements for sources of radiation in high-resolution molecular spectroscopy: continuous-wave emission, high modal power, low optical noise and high wavelength tunability [3]. The rapid tunability of these lasers is an important property that can be used in the study of chemical reactions, monitoring of fast processes or detection of molecular ions or short-lived radicals [3]. The spectral width of the lasers and the relatively high intensity of the emitted radiation form the basis for potential applications in sub-Doppler spectroscopy [4–7].

The development of technology has permitted the preparation of tunable lasers working in the C–H, N–H and O–H stretch-vibration regions (3.2–3.6 μm). Yakovlev and coworkers [3] and Martinelli [8] introduced the commercial use of III–V lasers. Because a smooth waveguide is formed in the cavity, lower noise is expected from competing modes in InAsSb/InAsSbP-based lasers with controlled injection density across the cavity width. In this type of laser, the nonequilibrium carrier concentration rises from the middle

of the cavity towards its ends. This forms a smooth waveguide across the cavity in which the radiation flux oscillates from one cavity edge to the other and back. Therefore, energy accumulation in the form of a nonequilibrium carrier concentration in the different parts of the cavity can be prevented. Consequently, emission of this energy in the form of radiation over a wide mixed spectrum is avoided.

In previous papers [9–11], we demonstrated that lasers with a smooth waveguide yield a narrow spectral line width  $\Delta f$ . Study of the dependence of the laser line width on the structural properties of the laser crystal indicated that small differences in  $\Delta f$  in all the lasers are not caused by defects in the crystals or random defects, but rather by physical processes involving interactions of the radiation with nonequilibrium charge carriers. Because the carrier concentration and the corresponding refractive index fluctuate,  $\Delta f$  depends primarily on these parameters. The proposed theoretical model [10] yields values of line width from three to 10 times greater than those predicted by Henry [12] and Yamada [13]. Consideration of the physical processes taking place in the tunable lasers with a smooth waveguide of different geometric parameters suggests a heavy dependence of the lasing line width on both the concentration of nonequilibrium charge carriers  $N$  and the volume of the active region [10].

This article is concerned with the production and testing of InAsSb/InAsSbP lasers emitting at a frequency range 3232–3238 cm<sup>-1</sup>, which operate in the temperature range 15–80 K. It can be expected that this type of laser has a narrower spectral line width  $\Delta f$  than lasers described in earlier works [9–11] and can be used as a radiation source for sub-Doppler spectroscopy.

### 2 Structure of the laser diodes

The main part of the diode lasers consisted in an InAsSb/InAsSbP double heterostructure grown by liquid-phase epitaxy on *p*-InAs(100) substrates doped with Zn with a hole concentration of 10<sup>19</sup> cm<sup>-3</sup>, as described in [14, 15]. The charge-carrier concentrations in the individual layers and the geometric parameters of the structure were selected so as to permit the laser operation at low temperatures whilst simultaneously keeping the carriers from being frozen out. The

✉ Fax: +420-286/591-766, E-mail: civis@jh-inst.cas.cz

narrow-band InAsSb active layer with 0.4-eV band-gap energy at 77 K was 0.8–1.5- $\mu\text{m}$  thick and a formed the first type of heterojunction (2- $\mu\text{m}$  thick) with the InAsSbP cladding layers (the band-gap energy was 0.6 eV at 77 K). The electron concentrations in the doped layer were  $2\text{--}4 \times 10^{16} \text{ cm}^{-3}$ .

The zinc-doped *p*-InAsSbP cladding layer combined with the substrate had a hole concentration of about  $10^{19} \text{ cm}^{-3}$ . The *n*-InAsSbP cladding layer was doped by Sn and had an electron concentration of  $6\text{--}8 \times 10^{18} \text{ cm}^{-3}$ ; then the 0.5- $\mu\text{m}$ -thick InAs cap layer was doped by Sn with an electron concentration of about  $10^{19} \text{ cm}^{-3}$ . The thickness of the substrate was decreased to 100  $\mu\text{m}$  after epitaxial growth. The double-channel mesa-strip laser chips with 16- $\mu\text{m}$  strip width and 500- $\mu\text{m}$  step height were processed by photolithography. Laser diodes with a Fabry–Perot cavity length of 230–500  $\mu\text{m}$  were formed by cleaving. Laser chips were mounted on a special copper heat sink [14], which permitted the diode to be installed in a closed-cycle He Dewar.

### 3 Experimental

All the lasers were produced and their spectral characteristics were measured preliminarily in St. Petersburg at the temperature of liquid nitrogen. A detailed study of all the laser diodes was carried out in Prague using a diode-laser spectrometer described in detail in our previous papers [14–16].

#### 3.1 Measurement of the high-resolution spectra

The diodes were cooled using a closed-cycle He Dewar (Laser Photonics, model L573) working in the 12–100-K temperature regime. The laser radiation was focused by a toroidal mirror into a Czerny–Turner monochromator, which was used to suppress parasite laser modes. The radiation leaving the monochromator was directed either to an absorption cell filled with the absorbing gas and/or into a reference etalon with  $0.026 \text{ cm}^{-1}$  free spectral range. The actual cell was fitted with KBr windows and filled with the reference gas at an overall pressure of 3 Torr. The radiation intensity was measured using an InSb detector cooled with liquid nitrogen. The electric signal from the detector was amplified by a broad-band amplifier. The absorption spectra were measured using internal modulation of the laser at a frequency  $f$  of about 1 kHz in the current interval 50–300 mA. The signal was demodulated at  $2f$  using a lock-in amplifier and subsequently processed using a PC.

#### 3.2 Measurement of the laser line width

The technique of direct measurement of the absorption signal was used for estimation of the line width  $\Delta f$ . The laser was demodulated at a frequency of 200 Hz and the high-resolution spectrum of the reference gas was directly accumulated using a Le Croy 9361 digital oscilloscope (Fig. 1a) as signal  $U$  (at least 100 accumulations, Fig. 1a). The  $RC$  circuit with the time constant of 20  $\mu\text{s}$  differentiates the low-frequency part of the signal and transmits its high-frequency part  $U_R$  without distortion (Fig. 1b) [11]. The output voltage  $U_R$  is related to the input voltage  $U$  by the

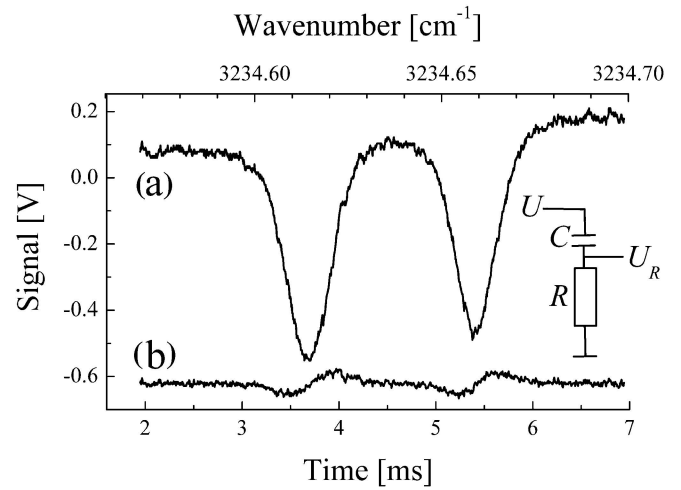


**FIGURE 1** Time dependence of functions. (a) Signal  $U(t)$  – absorption spectrum of the reference gas and (b) signal  $U_R(t)$  after filtering of the  $RC$  term, magnified five-fold for  $\text{NH}_3$  doublet. In the *inset* the  $RC$  circuit for modification of the signal  $U$  is shown

expression:

$$\frac{dU}{dt} = \frac{dU_R}{dt} + \frac{U_R}{\tau}, \quad (1)$$

where  $\tau = RC$  is the time constant of the  $RC$  circuit. The lasing frequency  $f = f_0 + \mu \cdot f_0$  continuously varies with the current, and  $\mu$  corresponds to the random deviations due to the variations in the current. The random deviations of the frequency  $\mu$  are responsible for the effective width of the lasing line. In view of the Lorentzian shape of the line [13],  $\Delta f$  can be found as the doubled standard deviation of the lasing frequency:

$$\Delta f = 2 \langle \mu \rangle. \quad (2)$$

The resistor voltage  $U_R$  contains the average component  $\bar{U}_R$  and the random quantity  $U_\mu$ . When averaging the  $U_R$  signal at extreme points, the  $d\bar{U}_R/dt$  value may be considered as zero. Since the result of averaging random quantities is always zero, we obtain:

$$U_R = \tau \frac{df_0}{dt} \frac{dU}{df}. \quad (3)$$

The signals with frequencies below  $1/\pi\tau$  are suppressed by the  $RC$  circuit. Therefore, the term  $U_\mu/\tau$  can be omitted from the  $dU/dt$  signal in the presence of components with much higher frequencies. Then, for the random components, we obtain after integrating (4):

$$\langle U_\mu \rangle = \frac{dU}{df} \langle \mu \rangle. \quad (4)$$

Substituting (4) and (3) into (2), we obtain (5), which was used for the calculation of  $\Delta f$ :

$$\Delta f = 2\tau \frac{df_0}{dt} \frac{\langle U_\mu \rangle}{\bar{U}_R}. \quad (5)$$

To measure the line width  $\Delta f$ , the tunable laser was energized by a direct current modulated by a saw-tooth current

with a modulation depth of 3–10 mV and a frequency of 200 Hz.

#### 4 Experimental results

The studied lasers could be divided into two groups: the emitting modes are produced by tuning of the laser current for one type of laser, while the laser wavenumber does not change for the others. Up to 10 emission modes were found in the spectra of the tunable lasers, corresponding to the resonator longitudinal mode. Moreover one or two space transverse modes may be situated near every longitudinal mode. At low current the predominance of the long-wavelength modes over the short-wavelength modes increased. The length of the resonator of the untunable lasers (300–500  $\mu\text{m}$ ) was statistically greater than for the tunable lasers (200–300  $\mu\text{m}$ ). The active-layer thickness of the untunable lasers (0.8–1.1  $\mu\text{m}$ ) was less than for the tunable lasers (1.0–1.5  $\mu\text{m}$ ).

When the input current  $I$  exceeded slightly the threshold current value  $I_{\text{th}}$  (from one- to three-fold) or was more than eight-fold higher, the emission spectrum of the tunable laser usually consisted of a series of modes. In the case where the current value lay between the above values (about four- to eight-fold), a single tuning mode dominated, and generally had a shorter wavelength. The threshold value of the tunable mode current  $I_{\text{tun}}$  increased relatively more slowly with increasing temperature (Fig. 2a) in contrast to the temperature dependence of the laser generation threshold current  $I_{\text{th}}$  (Fig. 2b). At current values near  $I_{\text{tun}}$ , the tunable laser mode is burned.  $I_{\text{tun}}$  and  $I_{\text{th}}$  were estimated by application of an external Ge etalon and the dependence of obtained signal (fringes of the etalon) on laser current drive (Fig. 3). The absence of fringes below  $I_{\text{th}} = 110$  mA indicates that there is no output signal at low currents. The largest tuning interval (up to  $6\text{ cm}^{-1}$ ) was achieved at temperatures of 15–20 K. At higher temperatures, this interval became narrower, especially as a consequence of the reformation of oscillations of the long-wavelength mode. At temperatures of more than 70–80 K, the single-mode regime could be observed only in the pulse regime, on short saw-toothed im-

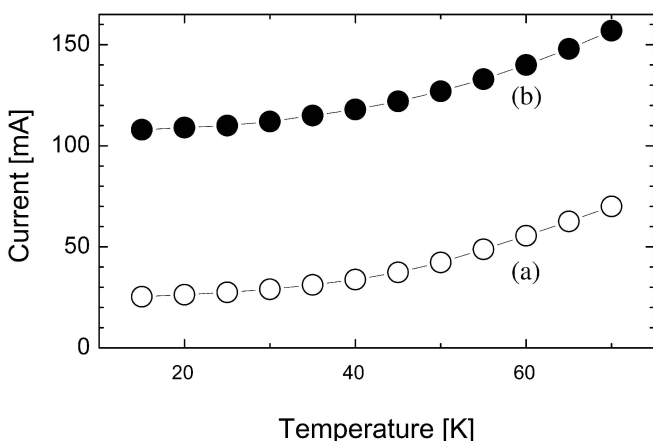


FIGURE 2 The temperature dependence of laser threshold current  $I_{\text{th}}$  (a) and tunable mode current  $I_{\text{tun}}$  (b)

pulses with a length of less than 20  $\mu\text{s}$  and a delay of 50  $\mu\text{s}$ . Figure 4 depicts the absorption spectra of  $\text{NH}_3$  obtained at a temperature of 17.5 K in the interval of current values from 110 to 350 mA. On the basis of the wavenumber of the identified absorption lines, a dependence was observed between the wavenumber of the generated radiation and the laser current (Fig. 5). The calibration dependence obtained approaches linearity.

The same rotation–vibration lines of  $\text{NH}_3$  were used for determining the laser line width. The use of preamplifiers with variously broad bands 10–80 and 80–300 kHz) yielded ap-

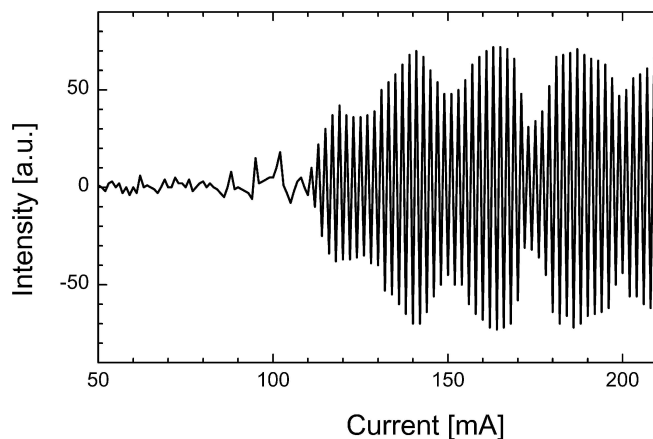


FIGURE 3 The intensity transmitted through the external Fabry–Perot resonator versus injection current

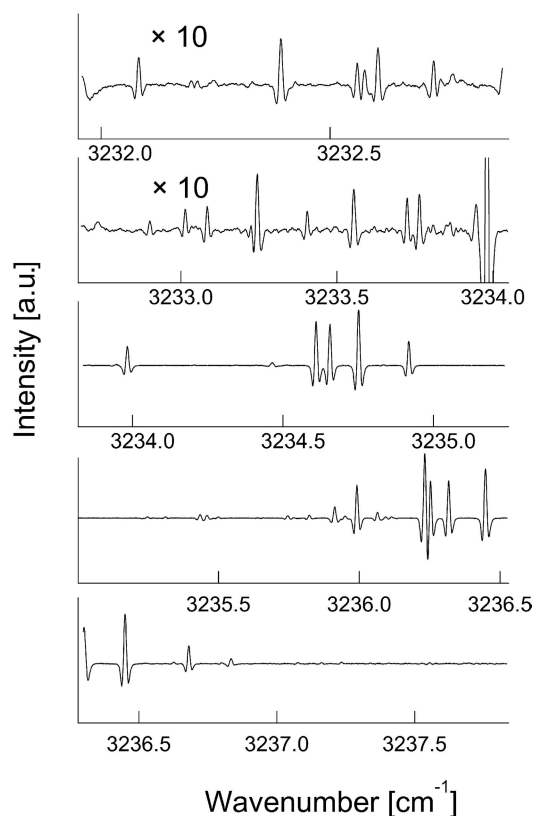
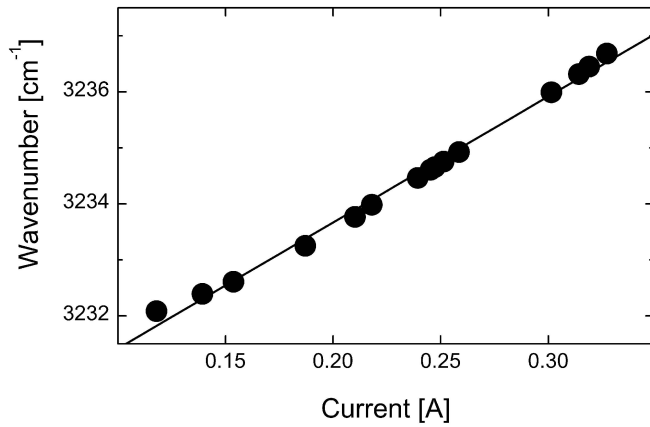
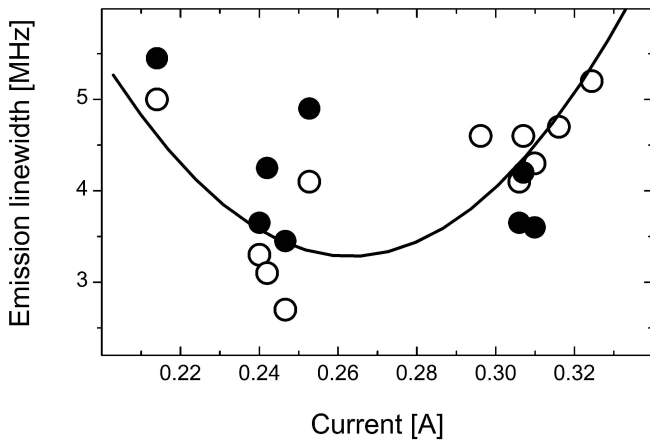


FIGURE 4 The absorption spectrum of  $\text{NH}_3$  obtained at laser temperature of 17.5 K



**FIGURE 5** The dependence of laser emission wavenumber on current, based on measurement of  $\text{NH}_3$  (Fig. 4)



**FIGURE 6** The spectral line width dependence on current obtained with amplifiers with different bandwidths. *Black circles* – 300 kHz, *open circles* – 80 kHz

proximately the same values of the laser line width, to within the experimental error (Fig. 6), under identical current conditions. For theoretical reasons, the measured experimental values were fitted with a parabola with a minimum at a current value of 270 mA and a laser line half-width of 7 MHz. This value is 1.4 times less than the value obtained in the previous works [9–11] for a similar type of laser. The lasers tested formerly had a lower concentration of acceptors in the substrate and in the confining layer and a smaller thickness of the active layer. The line widths were measured at higher temperatures (60–70 K) only. The increase in the concentration of holes in the limiting  $p$ -layer of the laser and the increase in the thickness of its active area thus permitted the production of a single mode tuning laser with narrow line width at low temperatures.

## 5 Discussion

The concentration of nonequilibrium charge carriers  $N$  in the current-tunable lasers rises with increasing current at current values exceeding the threshold value  $N_{\text{th}}$ . An increase in the concentration of charge carriers leads to a decrease in the refractive index  $n$ , because  $\partial n/\partial N < 0$ , as well as to an increase in the intrinsic frequencies of the laser resonator. The dependence of  $N$  on a change of the laser fre-

quency  $\Delta f$  is approximately expressed by (6):

$$N = N_{\text{th}} - n \frac{\Delta f}{f} \frac{\partial N}{\partial n}. \quad (6)$$

At the same time, the fluctuation of  $N$  leads to a frequency fluctuation of the laser resonator and to an increase in line width  $\Delta f$ . Taking into account the fluctuation of  $N$  by laser generation, the line width can be calculated by (7):

$$\Delta f = \frac{\tau_L f}{\tau_0 n} \left( \frac{8N}{V} \right)^{1/2} \left| \frac{\partial n}{\partial N} \right|. \quad (7)$$

$\tau_L/\tau_0$  is the ratio of the charge-carrier lifetimes for small deviations of  $N$  from the equilibrium state in the presence and absence of the laser radiation, and  $V$  is the volume of the active area. The ratio  $\tau_L/\tau_0$  in (7) also depends on  $N$ . For an intermediate degree of excitation that occurs in lasers at low temperatures,  $\tau_L/\tau_0$  and  $\partial n/\partial n$  can be calculated as follows [20]:

$$\frac{\tau_L}{\tau_0} = \frac{I_{\text{th}} (N - N_0) 2N_{\text{th}} + N_d}{IN_{\text{th}}B} \frac{2N_{\text{th}} + N_d}{N_{\text{th}} + N_d} \quad (8)$$

and

$$\frac{\partial n}{\partial N} = - \frac{1.15cA\sqrt{T} \sqrt{\frac{F_i}{kT}}}{6\pi^2 f (N_i + N_d)}. \quad (9)$$

$N_0$  is the inverse concentration of nonequilibrium charge carriers for the emission mode,  $F_i$  and  $N_i$  are the depths of Fermi-level occurrences and the concentrations of nonequilibrium charge carriers in the conduction region at the occupancy threshold, respectively,  $N_d$  is the concentration of donors,  $c$  is the speed of light,  $A = 186 \text{ cm}^{-1} \text{ K}^{-0.5}$  is a ratio defining the edge steepness in the active region and  $B$  is a ratio approximating 1 with up to 10% variation. The dependence of  $\Delta f$  on  $N$  and  $I$  (10) can be derived from (7–9):

$$\Delta f = \left( \frac{8NF_i}{VkT} \right)^{0.5} \frac{1.15cA\sqrt{T}}{6n\pi^2 (N_i + N_d)} \frac{I_{\text{th}}}{I} \frac{N - N_0}{N_{\text{th}}B} \frac{2N_{\text{th}} + N_d}{N_{\text{th}} + N_d}. \quad (10)$$

Equations (8–10) can explain the observed dependences of laser line width and tuning range on temperature and current. It follows from (8) that  $\tau_L/\tau_0 = 1$  at  $I = I_{\text{th}}$  and decreases with current, thus promoting the damping of the random fluctuations of the density of nonequilibrium carriers and smoothing the fluctuations of the refractive index. Equation 9 implies a decrease in  $\partial n/\partial N$  with the donor concentration because  $F_i$  increases more slowly than  $N_d$ . As a result, the presence of donors narrows the range of the lasing frequency modulation.

Equation 10 suggests that there are two main causes of the decrease in  $\Delta f$  with the lowering of temperature: one is the decrease in  $N$  that is proportional  $T^{3/2}$  [17], and the other is an increase in  $I/I_{\text{th}}$  in the frequency-tuning mode. The latter statement requires special comment.

According to our results [17–19], the smooth optical waveguide results from accumulation of nonequilibrium

charge carriers at the ends of the resonators. Exceeding of the current-carrier concentration above its threshold value is temperature-independent in a first approximation.  $N_{\text{th}}$  decreases with decreasing temperature and thus it is necessary to use a larger ratio  $I/I_{\text{th}}$  at lower temperatures in order to attain the necessary level of the carrier concentration. When the current slightly exceeds the threshold value, the actual generated modes can be tuned, as seen in Fig. 3. The frequency is tuned only at more than a four-fold current excess over  $I_{\text{th}}$  at a temperature of 17.5 K (Fig. 2 and 3). In addition, these considerations also explain the  $I_{\text{tun}}/I_{\text{th}}$  decrease with temperature rise (Fig. 2).

Recording of the vibration-rotation spectrum of  $\text{NH}_3$  (Fig. 4) led to the threshold value of four- to 13-fold excess, in accordance with (10). The absorption lines of ammonia were measured with a precision of  $0.002 \text{ cm}^{-1}$  and a calibration curve of the dependence of the wavenumber on the current was drawn up using the rotation-vibration lines (Fig. 5). The laser line width was determined on the strongest lines of ammonia in the current interval 210–330 mA (Fig. 6). The experimental  $\Delta f$  values are close to the values calculated according to (10).

The tendency for a decrease of the  $\Delta f$  values with current increase (at low flow rates) is connected with a decrease in the differential lifetime of the charge carriers  $\tau_L/\tau_0$ . The tendency for an increase of  $\Delta f$  with increasing current (at high flow rates) may be linked to the concentration increase of nonequilibrium charge carriers  $N$  in the frequency-tunable lasers. A decrease in the working temperature of the frequency-modulated diode laser permits a narrower width of the emission line of the laser.

## 6 Conclusion

We manufactured and tested a new type of current-tuned InAsSb/InAsSbP laser with the structure that prevents freezing out of the carriers and ensures their operation at low temperatures. Cooling of the laser structure down to 15–20 K made it possible to reduce the lasing line width to 7 MHz. The lasers are tunable in the spectral region up to  $6 \text{ cm}^{-1}$  and can serve as radiation sources for high-resolution

laser spectroscopy and for monitoring of harmful gases in the atmosphere.

**ACKNOWLEDGEMENTS** The work was sponsored by the Grant Agency of the Academy of Science of the Czech Republic (Grant No. A-4040104), the Grant Agency of the Czech Republic (Grant No. 203/01/0634) and the Russian Fund of Fundamental Research (Grant No. 99-02-18019).

## REFERENCES

- 1 V.G. Avetisov, A.N. Baranov, A.N. Imenkov, A.I. Nadezhdinskii, A.N. Khushnutdinov, Y.P. Yakovlev: *Sov. Tech. Phys. Lett.* **16**, 66 (1990)
- 2 A.I. Nadezhdinskii: *Monitoring of Gaseous Pollutants by Tunable Diode Lasers In: Symp., Freiburg, 1991, ed. by R. Grisar, G. Schmidtke, M. Tacke, G. Restell (Kluwer, Dordrecht 1992) p. 155*
- 3 A.N. Baranov, A.N. Imenkov, V.V. Sherstnev, Y.P. Yakovlev: in *Proc. Fifth Int. Conf. InP Related Materials, Paris, 1993, p. 19*
- 4 C.E. Wiemann, L. Hollberg: *Rev. Sci. Instrum.* **62**, 1 (1991)
- 5 K.B. MacAdam, A. Steinbach, C. Wiemann: *Am. J. Phys.* **60**, 1098 (1992)
- 6 J. Gea-Banacloche, Y.G. Li, S.Z. Jin, M. Xiao: *Phys. Rev. A* **51**, 576 (1995)
- 7 M. Xiao, Y.G. Li, S.Z. Jin, J. Gea-Banacloche: *Phys. Rev. Lett.* **70**, 666 (1995)
- 8 R.U. Martinelli: *Laser Focus World* **3**, 77 (1996)
- 9 A.N. Imenkov, N.M. Kolchanova, S. Civiš, Y.P. Yakovlev, P. Kubát: *Semiconductors* **34**, 1406 (2000)
- 10 A.N. Imenkov, N.M. Kolchanova, P. Kubát, K.D. Moiseev, S. Civiš, Y.P. Yakovlev: *Semiconductors* **35**, 360 (2001)
- 11 A.N. Imenkov, N.M. Kolchanova, S. Civiš, Y.P. Yakovlev, P. Kubát: *Rev. Sci. Instrum.* **72**, 1988 (2001)
- 12 C.N. Henry: *IEEE J. Quantum Electron.* **QE-18**, 259 (1982)
- 13 M. Yamada: *IEEE J. Quantum Electron.* **QE-30**, 1511 (1994)
- 14 A.A. Popov, V. Sherstnev, Y.P. Yakovlev, S. Civiš, Z. Zelinger: *Spectrochim. Acta A* **54**, 821 (1998)
- 15 A.A. Popov, V. Sherstnev, Y.P. Yakovlev, S. Civiš, Z. Zelinger: *Sov. Tech. Phys. Lett.* **23**, 890 (1997)
- 16 A.A. Andaspaeva, A.N. Baranov, V.L. Gel'mont, B.E. Djurtanov, G.G. Zegrya, A.N. Imenkov, Y.P. Yakovlev, S.G. Yastrebov: *Semiconductors* **25**, 240 (1991)
- 17 A.P. Danilova, T.N. Danilova, O.Y. Ershov, A.N. Imenkov, V.V. Sherstnev, Y.P. Yakovlev: *Semiconductors* **32**, 339 (1998)
- 18 A.P. Danilova, T.N. Danilova, A.N. Imenkov, N.M. Kolchanova, M.V. Stepanov, V.V. Sherstnev, Y.P. Yakovlev: *Semiconductors* **33**, 924 (1999)
- 19 A.P. Astachova, T.N. Danilova, A.N. Imenkov, N.M. Kolchanova, V.V. Sherstnev, Y.P. Yakovlev: *Semiconductors* **34**, 1100 (2000)
- 20 P.G. Elysejev, A.P. Bogatov: *Phys. Inst. RAS Trans.* **166**, 15 (1986)